THE JOURNAL OF PHYSICAL CHEMISTRY B LETTERS

2006, *110,* 20115−20117
Published on Web 09/21/2006

Long-Lived Interfacial Vibrations of Water

Zhaohui Wang, Yoonsoo Pang, and Dana D. Dlott*

School of Chemical Sciences, University of Illinois at Urbana-Champaign, 600 S. Mathews Ave., Urbana, Illinois 61801

Received: June 24, 2006; In Final Form: July 27, 2006

We have observed long-lived OH-stretch (ν_{OH}) excitations ($v = 1$) in water during ultrafast laser ablation by a mid-infrared pulse tuned to the ν_{OH} absorption maximum. The spectrum of excitations is measured using incoherent anti-Stokes Raman spectroscopy. Relative to the equilibrium water spectrum, these excitations evidence a narrowed (100 cm^{-1} fwhm) and blue-shifted (3600 cm^{-1} peak) transition. The excited-state lifetime is $T_1 > 200$ ps, compared to 0.2 ps in bulk water. In the early stages of the ablation process, the water mean density decreases rapidly, which breaks up the hydrogen bonding. The long-lived species is attributed to ν_{OH} excitations on water molecules associated with interfaces, having broken hydrogen bonds which cannot be rapidly reformed as in the liquid state.

The OH-stretch excitations (ν_{OH}) of water have the shortest population relaxation lifetime, $T_1 = 0.2$ ps,[1−4] of any known condensed-phase vibrational fundamental. The rapid vibrational relaxation results from strong anharmonic coupling to an extensive hydrogen bonding network. About 40% of molecules of water in equilibrium have broken hydrogen bonds, which might (but does not) result in a subensemble with longer lifetimes. Vibrational energy does not stay for long on a molecule with broken hydrogen bonds; either the energy hops[5] to an adjacent molecule or the broken bonds quickly reform.

The motivation of the present work is to study vibrational relaxation in water during a massive disruption of the hydrogen bonding network. The disruption is caused by ultrafast laser ablation. In the ablation process, bulk water undergoes a rapid decrease in mean density as it transitions to an ablation plume of tiny water droplets. On the basis of laser ablation simulations, Zhigilei et al.[6] describe the state present at ∼200 ps as a "foamy transient structure of interconnected liquid clusters".

Water ν_{OH} vibrations at liquid−vapor or liquid−vacuum interfaces have been studied extensively by vibrational sum-frequency generation (SFG) spectroscopy[7,8] and by infrared (IR) cluster predissociation spectroscopy.[9] In both types of measurements, a sharper ∼20 cm^{-1} width feature is observed near 3700 cm^{-1}, which is attributed to free surface OH groups. Broader features are seen at lower wavenumbers that are attributed to various icelike and liquidlike structures and structures with broken hydrogen bonds.[7−9]

The technique used here[10,11] involves an IR pump pulse tuned to excite ν_{OH} of water and a time-delayed visible probe pulse that generates incoherent anti-Stokes Raman emission. The time decay of the incoherent anti-Stokes spectrum is a direct measure of T_1.[12] Ordinarily, one would not think of using Raman spectroscopy to study water interfaces. Raman would not discriminate against a bulk water background, and Raman is not sensitive enough for gas-phase cluster measurements. However, our novel experiments provide both sensitivity and selectivity. The sensitivity results from the use of a transient high-surface-area material created by laser ablation. The selectivity results from the large difference in T_1 between bulk ν_{OH} and the interfacial ν_{OH} observed here. After a few picoseconds, all bulk excitations have decayed, leaving only excitations associated with interfaces.

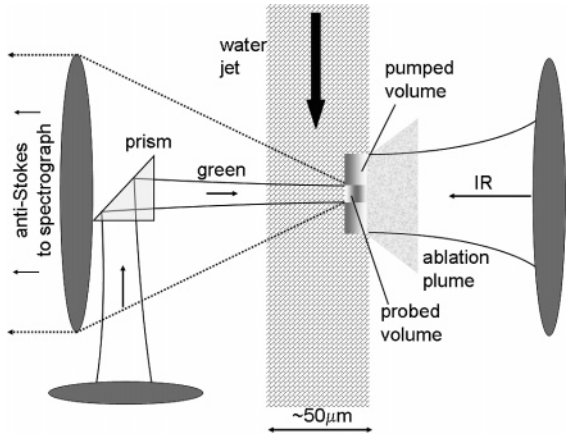

Figure 1. Optical arrangement with a water jet, and IR pump and green probe pulses. The transient anti-Stokes Raman spectrum of water during ultrafast laser ablation is observed with a spectrograph and CCD detector.

The experimental method and apparatus[10,11,13,14] have been described previously. The optical arrangement at the liquid water sample[11] is diagrammed in Figure 1. The pulses were generated by Ti:sapphire pumped optical parametric amplifiers operating at a repetition rate of 1000 Hz. The IR pump pulses at 3310 cm^{-1} had a duration of ∼1.0 ps, a bandwidth of ∼35 cm^{-1} and an approximately Gaussian spatial profile with ($1/e^2$) beam radius $r_0 = 150$ μm. The maximum IR pulse energy E_p was 43 μJ. The 10 μJ, 532 nm green probe pulses had a duration of

* To whom correspondence should be addressed. Electronic mail: dlott@scs.uiuc.edu.

10.1021/jp063962m CCC: $33.50

0.8 ps, a bandwidth of 25 cm^{-1}, and a beam radius $r_0 = 100$ μm. The smaller probe beam selectively probed water at the center of the pump beam.

As the pump pulse energy was increased, an ablation threshold was observed at $E_p \approx 30$ μJ. At threshold, a sudden increase in probe (green) light scattering, accompanied by large fluctuations, was observed along with a fine spray of droplets. The ablation measurements reported here were made a bit above threshold, at $E_p = 43$ μJ, where the ablation process was more stable. The tip of a pipet connected to a vacuum was placed near the water surface so that the droplets could be sucked away during the 1 ms interval between laser shots.

At 3310 cm^{-1}, the absorption coefficient of water is quite large, $\alpha = 4660$ cm^{-1},[15] so the pump pulse strongly heated a slab of water ~1 μm deep. Since water is transparent at 532 nm, the probe pulse investigated the pumped region along with a much larger volume of unpumped water, as shown in Figure 1. However, the concentration of ν_{OH} excitations at ambient temperature is very small, $n = [\exp(h\nu/kT) - 1]^{-1} = 10^{-7}$, so the observed signal originated entirely from ν_{OH} in the region excited by the pump pulse.

The water is heated nonuniformly[11] (see Figure 1) by the IR pulse of energy E_p, with the hottest region located at the sample surface at the center of the IR beam, where the incident fluence $J_c = 2E_p/(\pi r_0^2)$. The peak energy density E_v in the pumped volume of water is given by $E_v = J_c\alpha$. The vibrational excitations become thermalized within a few picoseconds,[1−3,16] and on this time scale, heating is both adiabatic and isochoric. The peak energy density at threshold is $E_v \approx 400$ J/cm^3, and in our measurements, $E_v = 570$ J/cm^3. As a point of reference, water at 25 °C would be heated to 100 °C with $E_v = 315$ J/cm^3, and water at 25 °C would be totally vaporized with $E_v = 2575$ J/cm^3. Thus, the ablation regime corresponds to weakly superheated water, where the IR pulses have enough energy to convert up to ~10% of the heated liquid to vapor.

The peak pressure and temperature jumps are[17]

$$\Delta T_{pk} = \frac{J_c\alpha}{\rho C_v} = \frac{2E_p\alpha}{\pi r_0^2 \rho C_v} \quad (1)$$

and

$$\Delta P_{pk} \approx (\partial P/\partial T)_V \Delta T = (\beta/\kappa_T)\Delta T \quad (2)$$

where β is the coefficient of thermal expansion and κ_T the isothermal compressibility. We assume we can use the ambient properties of water, $\rho C_v = 4.2$ J K^{-1} cm^{-3} and $(\partial P/\partial T)_V = 18$ atm K^{-1}, even into the weak superheating region. Then, at threshold where $E_p \approx 30$ μJ, $\Delta T_{thresh} = 95$ K and $\Delta P_{thresh} = 1.7$ kbar, and with $E_p = 43$ μJ, $\Delta T_{pk} = 135$ K and $\Delta P_{pk} = 2.4$ kbar. The pressure estimate is a lower limit, since it does not include the steam generated by the superheated water.

From the hydrodynamic point of view, the superheated water is a disk ~1 μm thick which is more than 100 μm in diameter. Driven by the kilobar internal pressure, the disk is driven away from the liquid surface[17] while simultaneously expanding, ultimately fragmenting into a fine mist of droplets. A good estimate of the material velocity is the speed of sound, which is ~1 km/s or 1 nm/ps, so at a time of ~200 ps, the disk thickness will have increased from ~1.0 to ~1.2 μm, and the disk may have cooled as well. Thus, the mean density decrease at 200 ps is ~20%. At the microscopic level, the expansion is not uniform; a vast number of microscopic nucleation sites are created where water vapor is generated. As time progresses and these nucleation sites expand, liquid−vapor interfaces are created leading to the "foamy transient structure" mentioned above.

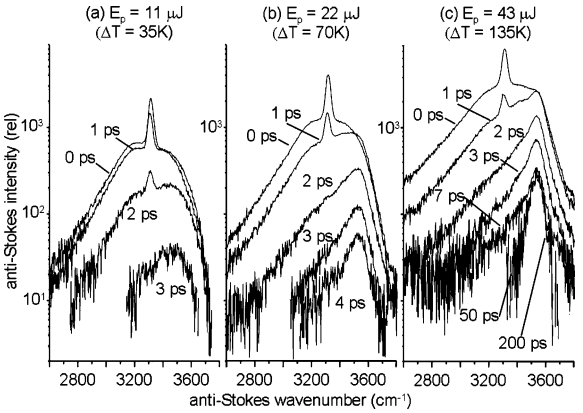

Figure 2. Transient anti-Stokes spectra with 3310 cm^{-1} pump pulses at the indicated energies. Water ν_{OH} excitations are created and detected. (a,b) Below the ~30 μJ ablation threshold, red-shifted excitations decay more quickly, leading to a time-dependent spectral blue shift. After ~5 ps, all ν_{OH} excitations have decayed. (c) Above the ablation threshold, a long-lived blueshifted spectrum is observed that persists beyond 200 ps.

Figure 2 shows anti-Stokes data in the ν_{OH} region on semilog axes, with a pump pulse (3310 cm^{-1}) tuned to the water absorption maximum. The sharper feature at 3310 cm^{-1} is a coherent artifact due to nonlinear light scattering.[10] It is a kind of weak SFG signal that arises from the bulk of the water sample (SFG is forbidden in the bulk only within the dipole approximation) that is present only when the pump and probe pulses overlap temporally.

Figure 2a−c compares results obtained with progressively higher intensity pump pulses. Each time the pulse intensity is doubled, the signal level also doubles. With $\Delta T = 35$ and 70 K (Figure 2a,b) the results are similar, and similar to what has been reported previously.[14,18,19] As time progresses, ν_{OH} excitations decay faster on the red edge, so that after a few picoseconds the remaining excitations are concentrated on the blue edge. It is well-known that in water there is a strong correlation between hydrogen bonding strength and frequency redshift.[20−22] These longer-lived ($T_1 = 0.8$ ps) blue-edge ν_{OH} excitations exist in regions where the hydrogen bonding has been weakened by the thermalization process.[23] After 3−4 ps, the ν_{OH} excitation level has dropped below our detection limit. With data obtained above the ablation threshold, as shown in Figure 2c, a new feature is observed. The anti-Stokes Raman spectrum of ν_{OH} excitations continues to narrow and blue-shift until about 10 ps. Subsequently, the spectrum, peaked near 3600 cm^{-1}, remains unchanged out to at least 200 ps. Judging from relative intensities, this long-lived excited-state ν_{OH} population comprises several percent of the initial excited states.

There can be no doubt that the 200 ps anti-Stokes signals in Figure 2c are associated with long-lived ν_{OH} ($v = 1$) excitations of water. If this spectrum were an artifact due to a nonlinear interaction between the pump and probe pulses, it would be centered at 3310 cm^{-1} and would disappear at time delays past 2 ps. The spectrum also has the wrong shape and wrong intensity to result from anti-Stokes scattering from equilibrium water heated by the pump pulse. The peak energy density $E_v = 570$ J/cm^3 corresponds to ~25% of the water molecules at the surface being excited to $v = 1$, so the long-lived spectrum in Figure 2c represents an occupation number $n \approx 5 \times 10^{-3}$. If this were due to ordinary heating processes, the temperature would have to be ~900 K, which is inconceivable.

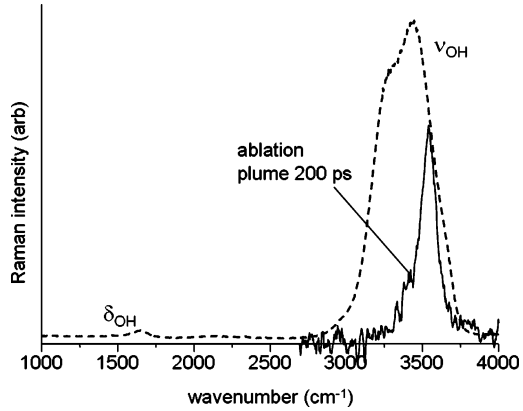

Figure 3. Comparison of the transient anti-Stokes Raman spectrum of the long-lived water ν_{OH} excitations observed during laser ablation with the equilibrium Stokes Raman spectrum of water.

We attribute the long-lived spectrum in Figure 2c to ν_{OH} excitations associated with the liquid−vapor interfaces created by the rapid expansion. The spectrum is too broad and too red-shifted to result from water vapor or isolated water molecules. The association of this spectrum with interfacial water follows from its appearance during ablation, from the blue shift in Figure 3 that indicates broken hydrogen bonds and from the weak coupling to the bath of bulk states implied by the enormous (>1000-fold) increase in T_1.

Measurements of T_1 such as those presented here could not be accomplished with SFG, even using femtosecond pulses. In a time-delayed SFG experiment,[24,25] the SFG signal decays with the coherence lifetime T_2 rather than the population lifetime T_1. From the inequality $T_2 \leq 2T_1$, coherence decay measurements can be used to set a lower limit to T_1,[12] but this is not very useful for room-temperature liquids where it is often the case that T_1 exceeds T_2 by orders of magnitude.[26]

In SFG studies of water−vapor interfaces, an ~20 cm^{-1} width peak at 3700 cm^{-1} is observed that is attributed to surface free OH groups.[7−9] We do not see such a feature, and we believe this is because both the spectroscopic methods and the interfaces are quite different in our experiments. SFG is believed to be sensitive only to the first layer of water molecules,[27] but IR−Raman does not have this type of interface selectivity. The long-lived water vibrations may be more than one layer below the interface. The interfacial regions in the early stages of the ablation process may involve thin layers of vapor sandwiched between liquid regions, and possibly thin layers of water sandwiched between vapor regions, and these water structures may be disordered due to the dynamical expansion and large curvature effects.

Features similar to the 100 cm^{-1} width transition at 3600 cm^{-1} shown in Figure 3 are frequently seen in SFG and water cluster studies. In the SFG literature of water−air interfaces,[7,8] these are described as resulting from the bonded OH stretch of surface water molecules with one bonded OH and one free surface OH. In the water simulation literature,[21,22,28] spectra have been computed for subensembles having different hydrogen bonding. Our spectra quite closely resemble water molecules having a non-hydrogen-bonded H atom plus a non-hydrogen-bonded O atom.[21] In other words, the transient spectrum in Figure 3 is best described as representing liquid-state water molecules with multiple broken hydrogen bonds. These bonds remain broken for much longer than in water, since within the ablation plume, the rapid volume expansion impedes hydrogen bond reformation.

In conclusion, we have observed long-lived ν_{OH} excitations in water during ultrashort laser pulse ablation. The lifetime is >200 ps, compared to the 0.2 ps lifetime in bulk water. In the early stages of the ablation process, the water undergoes a rapid mean density decrease which breaks up the hydrogen bonding, creating a dense foam with many interfaces embedded in liquid water. The ν_{OH} excitations on water molecules with broken hydrogen bonds have much longer lifetimes than in bulk water, because the broken hydrogen bonds cannot be reformed rapidly as in the bulk liquid.

Acknowledgment. This material is based on work supported by the National Science Foundation under award DMR-05 04038. Additional support was provided by the U.S. Air Force Office of Scientific Research under award number F49620−03−1−0032, and by the U.S. Department of Energy through the Stewardship Sciences Academic Alliance Program from the Carnegie-DOE Alliance Center under award no. DE-FC03-03NA00144.

References and Notes

(1) Lock, A. J.; Bakker, H. J. *J. Chem. Phys.* **2002**, *117*, 1708.
(2) Lock, A. J.; Woutersen, S.; Bakker, H. J. *J. Phys. Chem. A* **2001**, *105*, 1238.
(3) Cringus, D.; Lindner, J.; Milder, M. T. W.; Pshenichnikov, M. S.; Vöhringer, P.; Wiersma, D. A. *Chem. Phys. Lett.* **2005**, *408*.
(4) Cowan, M. L.; Bruner, B. D.; Huse, N.; Dwyer, J. R.; Chugh, B.; Nibbering, E. T. J.; Elsaesser, T.; Miller, R. J. D. *Nature (London)* **2005**, *434*, 199.
(5) Woutersen, S.; Bakker, H. J. *Nature (London)* **1999**, *402*, 507.
(6) Zhigilei, L. V.; Leveugle, E.; Garrison, B. J. *Chem. Rev.* **2003**, *103*, 321.
(7) Richmond, G. L. *Chem. Rev.* **2002**, *102*, 2693.
(8) Shen, Y. R.; Ostroverkhov, V. *Chem. Rev.* **2006**, *106*, 1140.
(9) Steinbach, C.; Andersson, P.; Kazimirski, J. K.; Buck, U.; Buch, V.; Beu, T. A. *J. Phys. Chem. A* **2004**, *108*, 6165.
(10) Deàk, J. C.; Iwaki, L. K.; Dlott, D. D. *J. Phys. Chem.* **2000**, *104*, 4866.
(11) Deàk, J. C.; Iwaki, L. K.; Rhea, S. T.; Dlott, D. D. *J. Raman Spectrosc.* **2000**, *31*, 263.
(12) Laubereau, A.; Kaiser, W. *Rev. Mod. Phys.* **1978**, *50*, 607.
(13) Pakoulev, A.; Wang, Z.; Pang, Y.; Dlott, D. D. *Chem. Phys. Lett.* **2003**, *380*, 404.
(14) Wang, Z.; Pakoulev, A.; Pang, Y.; Dlott, D. D. *J. Phys. Chem.* **2004**, *108*, 9054.
(15) Bertie, J. E.; Lan, Z. *Appl. Spectrosc.* **1996**, *50*, 1047.
(16) Huse, N.; Ashihara, S.; Nibbering, E. T. J.; Elsaesser, T. *Chem. Phys. Lett.* **2005**, *404*, 389.
(17) Hare, D. E.; Franken, J.; Dlott, D. D. *J. Appl. Phys.* **1995**, *77*, 5950.
(18) Pakoulev, A.; Wang, Z.; Dlott, D. D. *Chem. Phys. Lett.* **2003**, *371*, 594.
(19) Wang, Z.; Pakoulev, A.; Pang, Y.; Dlott, D. D. *Chem. Phys. Lett.* **2003**, *378*, 281.
(20) Bratos, S.; Leicknam, J.-C. *J. Chem. Phys.* **1994**, *101*, 4536.
(21) Lawrence, C. P.; Skinner, J. L. *Chem. Phys. Lett.* **2003**, *369*, 472.
(22) Rey, R.; Møller, K. B.; Hynes, J. T. *J. Phys. Chem. A* **2002**, *106*, 11993.
(23) Bakker, H. J.; Lock, A. J.; Madsen, D. *Chem. Phys. Lett.* **2004**, *384*, 236.
(24) Bordenyuk, A. N.; Benderskii, A. V. *J. Chem. Phys.* **2005**, *122*, 134713.
(25) Roke, R.; Kleyn, A. W.; Bonn, M. *Chem. Phys. Lett.* **2003**, *370*, 227.
(26) Fayer, M. D. *Ultrafast Infrared and Raman Spectroscopy*; Marcel Dekker: New York, 2000.
(27) Perry, A.; Niepert, C.; Space, B.; Moore, P. B. *Chem. Rev.* **2006**, *106*, 1234.
(28) Lawrence, C. P.; Skinner, J. L. *J. Chem. Phys.* **2002**, *117*, 8847.